CFD based flow and heat transfer analysis of various ribs in solar air heater duct by continuous ribs on absorber plate

Sitaram Sah
sah.sitaram319@gmail.com
Patel College of Science and Technology, Bhopal,
Madhya Pradesh

Amit Kumar
amitavit689@gmail.com
Patel College of Science and Technology, Bhopal,
Madhya Pradesh

ABSTRACT

This article is present for a detailed investigation of the design of solar air heater having rib roughness on the absorber plate by using the application of computational fluid dynamics (CFD). In this Solar air heater an absorber plate is made of 'Al' and roughened with transverse ribs due witch creates the turbulence in the flow of fluid (air) and increase the heat transfer from the absorber plate to the fluid. The quantity of heat transfer is depending on the Nusselt number. The nusselt number depends on surface heat transfer coefficient 'h'. Heat transfer coefficient strongly depends on the relative roughness height (e). Here ANSYS FLUENT v 14.5 is used to simulate fluid flow through a conventional solar air heater.

Keywords: *Solar air heater, turbulent flow, Nusselt number, ribs, Reynolds number, Pitch*

1. INTRODUCTION

The Solar air heater is one of the basic equipment through which solar energy is converted into thermal energy. A solar air heater is a type of heat exchanger which transfers solar radiation into heat energy. Solar air heaters, because of their simple designing, are cheap and most widely used as a collection device of solar energy. A solar air heater requires little maintenance. The solar air heater is a type of solar thermal system where the air is heated in a collector and either transferred directly to the interior space or to a storage medium. A conventional solar air heater generally consists of an absorber plate, a rear plate, insulation below the rear plate, transparent cover on the exposed side, and the air flows between the absorbing plate and rear plate. The air gets heated up while the absorber plate absorbs the heat. The hot air is drawn through the plates with a blower which is operated electrically.

The main applications of solar air heater are space heating, seasoning of timber, curing of industrial products and these can also be effectively used for curing/drying of concrete/clay building components. The other applications of solar air heater are drying of agro and allied products, food items such as fruits, vegetables, chilies, tea-leaves, fish, salt, etc. The solar air heater can be used in many industrial activities (drying/heating) such as chemical, pharmaceutical, limited areas of textiles and hosieries, tannery, edible oil, etc.

2. REVIEW OF PAST RESEARCH

Hari Raghavan. J and Rangu. P (2017) understood the thermal benefits of using a porous pin fin heatsink when compared to a conventional pin fin heatsink. The cross-section of the heatsink used in the analysis is square shaped. The Heatsink is to be analyzed numerically for natural convection assuming steady state condition. Finite volume method is considered for doing the thermal analysis using a Computational Fluid Dynamics tool called FloTHERM
.

Arun Kumar T P and Vijayaraghu B (2017) studied a numerical simulation of heat transfer in the rectangular fin type of heat sink under various operating conditions. The methodology is validated by analyzing the flow through the rectangular channel with heat transfer. It is observed that the introduction ribs enhance the heat transfer capabilities. The effect of flow velocities on the Nusselt number at various rib length (0.2mm, 0.3mm, 0.4mm, and 0.5mm) as well as diagonal pitches(1.25mm, 1.5mm, 1.75mm, and 2mm) have been quantitatively analysed. The analysis showed that rib length 0.5mm and diagonal pitch 1.25mm gives the highest enhancement in the heat transfer. The provisional of ribs also result in increases in the pressure drop through the passage. Hence it is necessary to optimize both heat transfer coefficient and pressure drop simultaneously.

Amit Garg et al (2017) researched on heat transfer and fluid flow characteristics in a channel in the presence of diamond-shaped baffles in the laminar flow regime. The computations are based on the finite volume method, the Navier Stokes equations along

with the energy equation have been solved by using SIMPLE Technique. The unstructured triangular mesh is used for the computational domain. The fluid flow and heat transfer characteristics are presented for Reynolds numbers based on the hydraulic diameter of the channel ranging from 100 to 600. Effects of different baffle tip angles on heat transfer and pressure loss in the channel are studied and the results of the diamond baffle are also compared with those of the flat baffle. The velocity profiles were obtained for all the geometry considered and selected for different sections, namely, downstream and between the two baffles and the friction coefficients were obtained for different sections and for different Reynolds numbers. It is observed that apart from the rise of Reynolds number, the reduction of the baffle angle leads to an increase in the Nusselt number and friction factor.

K. Maliwan (2017) studied the flow and heat transfer characteristics in a rotating two-pass square channel with ribbed walls. In this study, the channel length-to-hydraulic diameter ratio of the rotating two-pass square channel (L/Dh), the rib height-to-hydraulic diameter ratio (e/Dh), rib angle of attack and the rib pitch-to-height (p/e) ratio are fixed at 11.33, 0.13, 60o and 10, respectively. The test fluid is air having the flow rate in terms of constant Reynolds number (Re) of 10,000. The rotation numbers (Ro) are varied from 0.1 to 0.4. The details of the local heat transfer distribution and the flow field of the rotating two-pass square channel are numerically studied by using commercial software ANSYS Fluent (ver.15.0).

3. COMPUTATIONAL DOMAIN
A rectangular section was considered. It consisted of three sections, test section of length L2 (1000 mm), entrance section of length L1 (500 mm) and exit length of length L3 (500 mm). The geometry taken is similar to that of Dongxu Jin et al [15] rectangular duct. Their rectangular duct was of length 2000 mm, width 300 mm and 30 mm height with a test section length of 1000 mm.

Fig. 1 shows the geometry of the computational domain. No rib and different rib arrangements employed for simulation are indicated in Fig. 2.
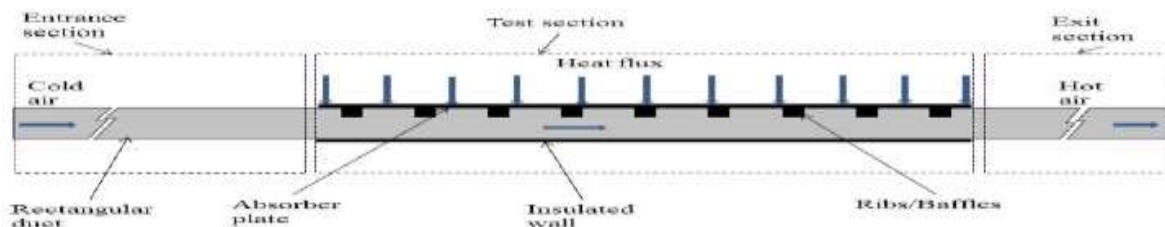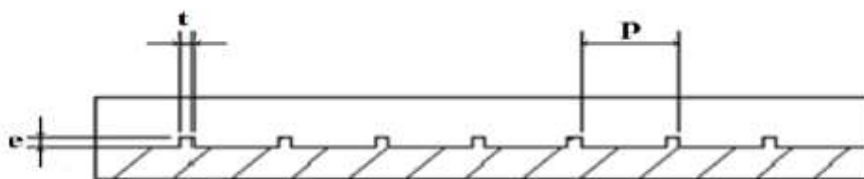

Fig. 1: Sketch of the computational domain

Fig. 2: Rib dimensions

Table 1: Operating and Geometrical parameters used for CFD analysis

Operating and Geometrical parameters	Value / Range
Test length of duct, L2	1000 mm
Entrance length of duct L1	500 mm
Exit length of duct L3	500 mm
Duct height, H	30 mm
Duct width, W	300 mm
Duct hydraulic diameter, Dh	54.54 mm
The aspect ratio of the duct, W/H	10
Constant heat flux, q	1000 w/m^2
The range of Reynolds number	2000-12000

Repeated square ribs (tt = 6 mm) and thin ribs (TB = 0.5 mm) with an axial pitch of p = 40 mm characterized the roughness parameters of the test duct. Re was varied from 2000-12000. Constant heat flux of value approximately 1000 W/m2 was supplied only on the upper wall of the absorber plate. Simulations were performed assuming the flow to be steady. The operating and geometrical parameters used for computational analysis are listed in Table 1.

4. RESULTS AND DISCUSSION
4.1 Effect of variation of pitch on artificial roughened wall
Most of the flow which occurs in practical applications are in general turbulent in nature. In the turbulent region, the velocity of the particles very near to surface becomes almost zero. In this region, the particle has very low kinetic energy. This region is called laminar sub-layer. These laminar sub-layer acts as a barrier of heat transfer from heated surface to the fluid medium. As shown in the Fig.3 ribs are attached underside of the absorber plate these ribs breaking and disturbing the laminar sublayer and flow is wavy flow.
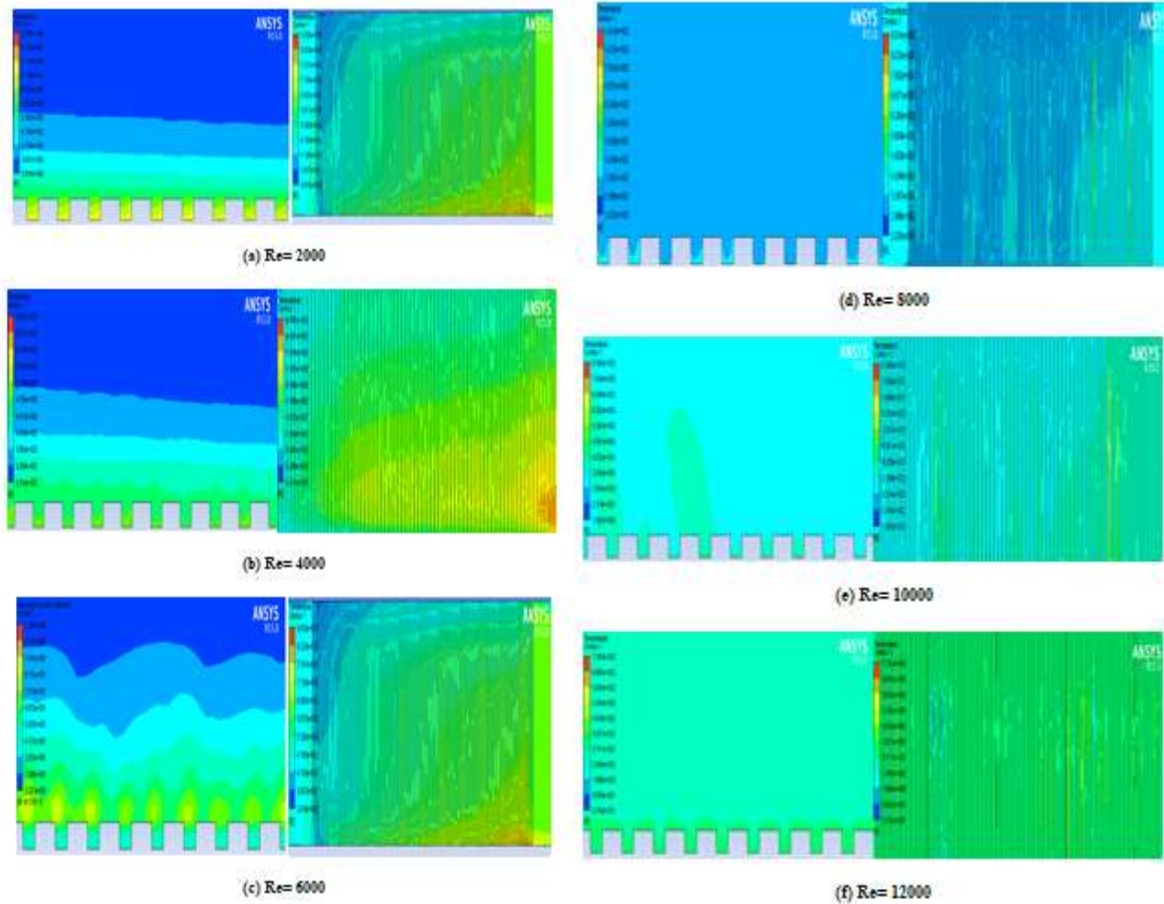
(a) Re= 2000

(d) Re= 8000

(b) Re= 4000

(e) Re= 10000

(c) Re= 6000

(f) Re= 12000

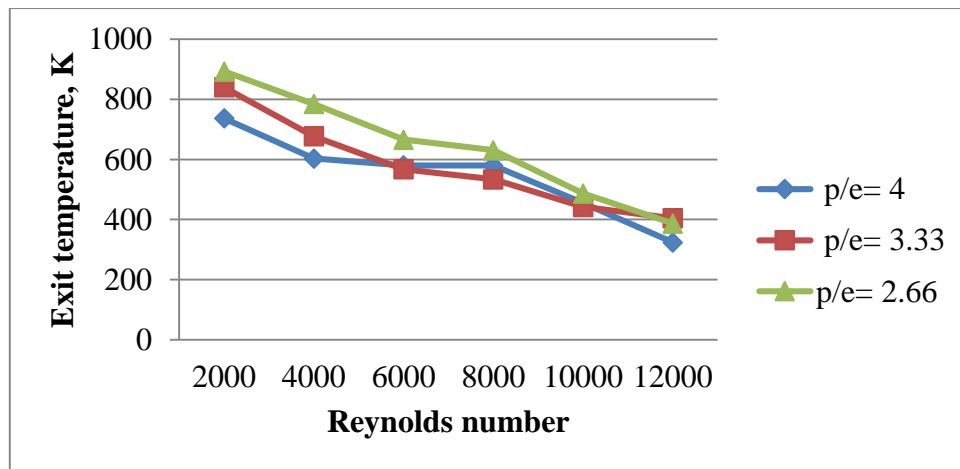**Fig. 3: Temperature contour plot at different Reynolds number for p/e= 2.66**

Fig. 4: Variation of the roughened plate for different values of temperature of the air at the exit of duct for p/e= 2.66

Figure 4 shows the variation of the temperature of the air at the exit with Reynolds number. As the Reynolds number increases, the heat carrying capacity of air increases. Because of this heat utilization also increases, but the rate of increase of heat capacity is more significant than the rate of increase of heat utilization. Therefore the temperature of the air at exit decreases as a result increase in Reynolds number.

Table 2: Air exit temperature at various Reynolds no. for roughen duct for p/e= 4, p/e = 3.33 and p/e = 2.66

S.No	Reynolds no.	Air exit temperature, K (p/e = 4)	Air exit temperature, K (p/e = 3.33)	Air exit temperature, K (p/e = 2.66)
1	2000	737.32	840.01	893.44
2	4000	603.47	677.12	785.68
3	6000	580.78	567.36	666.41
4	8000	580.11	534.10	631.87
5	10000	455.14	442.19	487.36
6	12000	324.23	504.52	387.68

4.2 Effect of Reynolds number on convective heat transfer coefficient for roughened wall

Figure 5 shows the variation of convective heat transfer coefficient with Reynolds number. As the Reynolds number increases, the heat transfer coefficient also increases for different values of relative roughness pitches. The variation in heat transfer coefficient is low at small Reynolds numbers while it is large at higher Reynolds numbers. This behavior seems due to increased turbulence at higher Reynolds numbers and also due to breakage of the thermal boundary layer at higher Reynolds numbers.
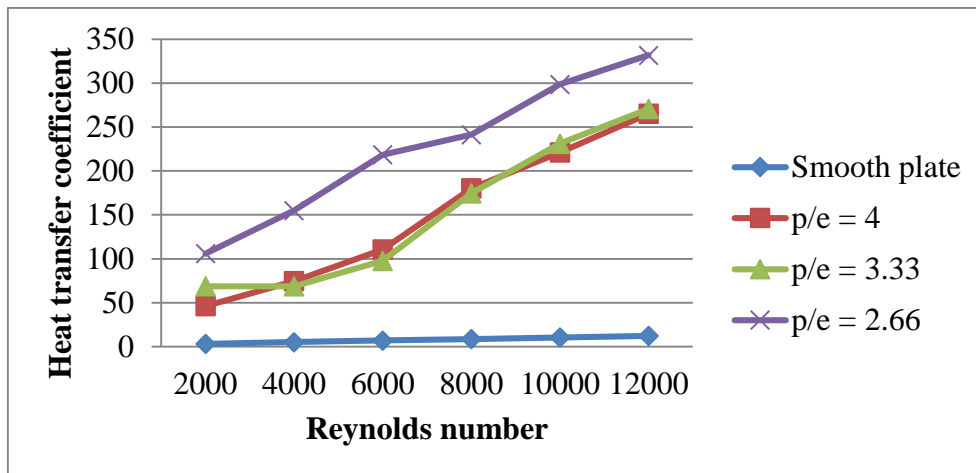

Fig. 5: Variation of heat transfer coefficient for smooth plates for different values of Reynolds number for p/e= 2.66

Table 3: Heat transfer coefficient at various Reynolds no. for roughen duct for p/e =4, p/e= 3.33 and p/e = 2.66

S.No	Reynolds no.	Heat transfer coefficient, W/m²K (Smooth duct)	Heat transfer coefficient, W/m²K (p/e =4)	Heat transfer coefficient, W/m²K (p/e = 3.33)	Heat transfer coefficient, W/m²K (p/e = 2.66)
1	2000	3.32	46.25	68.82	106.087
2	4000	5.33	74.63	68.82	154.96
3	6000	7.15	110.8	97.78	218.55
4	8000	8.66	180.31	174.61	241.35
5	10000	10.48	221.14	231.06	298.49
6	12000	12.42	265.2	270.74	331.72

4.3 Effect of Reynolds number on nusselt number

Figure 6 shows the variation of Nusselt number with Reynolds number. As the Reynolds number increases, the Nusselt number also increases for different values of relative roughness pitches. The variation in Nusselt number is low at small Reynolds numbers while it is large at higher Reynolds numbers due to breakage of the thermal boundary layer at higher Reynolds numbers and large turbulence.
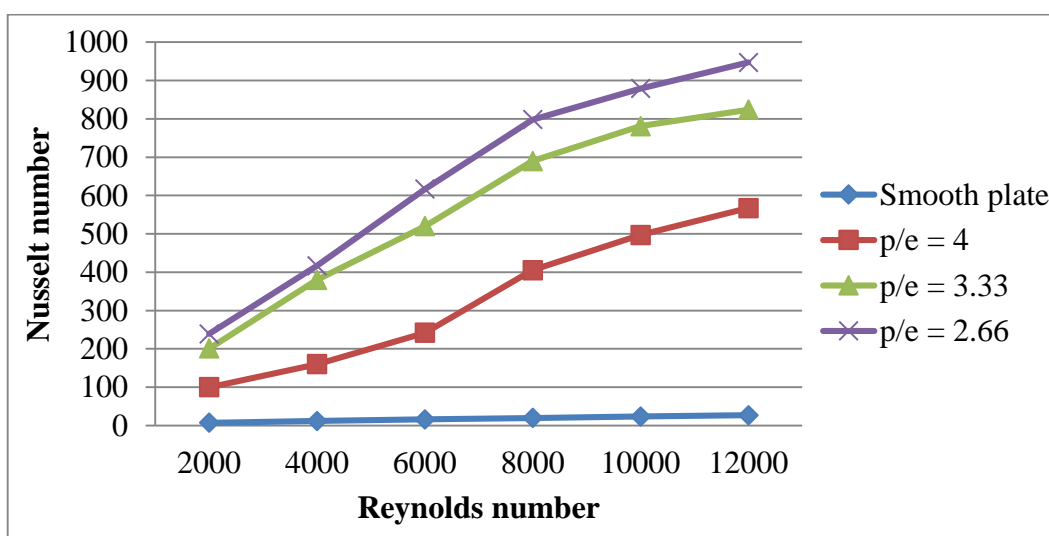

Fig. 6: Variation of nusselt number for smooth and roughened plate for different values of Reynolds number for p/e= 2.66

Configurations with p/e = 4, 3.33 and smooth duct exhibited similar trends in the increase of Nu with the velocity at the inlet. In contrast to that, a configuration with the smooth duct showed the lesser slope of variation in Nusselt number at the higher inlet velocities. In general, for a considerable range of inlet velocities, it can be observed that configurations with narrowly placed ribs exhibited lesser heat transfer and configurations with broadly placed ribs exhibited higher heat transfer.

Table 4: Nusselt no. at various Reynolds no. for roughen duct for for p/e =4, p/e= 3.33 and p/e = 2.66

S.No	Reynolds no.	Nusselt no. (smooth duct)	Nusselt no. (p/e = 4)	Nusselt no. (p/e = 3.33)	Nusselt no. (p/e = 2.66)
1	2000	7.48	100.11	201.11	239.09
2	4000	12.01	160.01	380.65	417.11
3	6000	16.11	242.23	520.78	617.32
4	8000	19.97	405.77	690.47	798.61
5	10000	23.62	497.65	781.56	879.44
6	12000	27.04	567.42	824.78	947.23

5. CONCLUSIONS

A three-dimensional CFD study was done to predict the influence of transverse rectangular cross-sectioned ribs on a solar air heater's convective heat transfer properties. A rectangular duct was constructed and CFD analysis was carried out on square and thin (high aspect ratio) rib shapes. The air was the working fluid and constant heat flux was applied only on the absorber plate's top surface. The output of simulations drew the following conclusions:

1. Based on the analysis, it has been found that the performance of solar air heater can be enhanced by providing artificial roughness in the form of ribs on the underside of the absorber plate than the conventional flat plate solar air heater.
2. From the analysis, it is observed that rate of heat transfer and pressure drops will be higher with the insertion of ribs in comparison with those of simple channels without the ribs.
3. For all the rib spacing, pitch 4 mm, pitch 3.33 mm and pitch 2.6 mm resulted in higher rate of heat transfer with relative increase in the pressure drop.
4. With all the cases considered ribs with pitch = 2.66 mm showed a maximum rate of heat transfer with maximum pressure drop throughout the entire range of input velocities considered.
5. Higher velocities near the wall and higher turbulence-induced mixing in staggered arrangement contribute towards better convective conditions and higher pressure drop in comparison with the inline arrangements.
6. The most important effect produced by the presence of a rib on the flow pattern is the generation of two flow separation regions, one on each side of the rib. The vortices so generated are responsible for the turbulence and hence the enhancement in heat transfer as well as in the friction losses takes place. A considerable influence of the presence of ribs is more pronounced in turbulence intensity distribution.
7. The nusselt number has been found to be highest for an absorber plate having relative roughness pitch equal to 8 mm.
8. For all the cases considered in this study, increase in Reynolds number leads to augmentation in Nusselt number.
9. CFD results have been also validated the smooth duct and different CFD model results were compared with the Dittus-Boelter empirical relationship for a smooth surface.
10. The results revealed that the thin ribs yielded better performance than the squared ones.
11. Similar results were also observed by Skullong et al. [16] in their experimental work.

6. REFERENCES
[1] Hari Raghavan. J, Rangu. P (2017), "A Study and Analysis on the Thermal Performance of a Pin Fin Heatsink for Natural Convection using CFD", International Journal of Engineering Research & Technology, 6 (5), PP: 883-888.
[2] Arun Kumar T P, Vijayaraghu B (2017), "Three Dimensional Numerical Analysis of Heat Transfer by Forced Convection through Heat Sink with Rectangular Ribs", International Journal of Modern Trends in Engineering and Research, 5 (1), PP: 238-243.
[3] Amit Garg, Sunil Dhingra, Gurjeet Singh (2017), "CFD Analysis of Laminar Heat Transfer in a Channel Provided with Baffles: Comparative Study between Two Models of Baffles: Diamond-Shaped Baffles of Different Angle and Rectangle", International Journal of Enhanced Research in Science Technology & Engineering, 3 (7), PP: 267-276.
[4] K. Maliwan (2017), "Numerical simulations on flow and heat transfer in ribbed two-pass square channels under rotational effects", Materials Science and Engineering, 5 (1), PP: 114-126.
[5] Mayank Bhola (2017), "Analysis of Heat Transfer of Ribbed Turbulent Channel using ANSYS", International Journal on Emerging Technologies, 8(1), PP: 236-242.
[6] Navanath .G.Ghodake, MRC. Rao, Dr. R. R. Arakerimath (2016), "Flow and Heat Transfer Analysis of Various Ribs for Forced Convection Heat Transfer", Journal of Emerging Technologies and Innovative Research", 3(7), PP: 42-47.
[7] S. V. Kadbhane, D. D. Palande (2016), "Review of Convective Heat Transfer from Plate Fins under Natural and Mixed Convection at Different Inclination Angle", International Research Journal of Engineering and Technology, 3 (2), PP: 467-473.
[8] C. H. Liang, S. Zeng, Z. X. Li (2016), "Optimal Design of Plate-Fin Heat Sink under Natural Convection Using a Particle Swarm Optimization Algorithm", International Journal of Heat and Technology", 34 (2), PP: 275-280.
[9] Nagaraju, B. Chandramohan Reddy (2016), "CFD Analysis of Flow and Heat Transfer in Solar Air Heater Duct by using V-Shaped Inclined Continuous Ribs on Absorber Plate", International Journal of Engineering Research & Technology, 5 (11), PP: 227-230.
[10] Swajot Singh, Raji N. Mishra (2016), "Evaluation of Convective Heat Transfer Coefficient at Different Altitudes in Atmospheric Regime Using Forced Convection", International Journal of Engineering Sciences & Research Technology, 5 (7), PP: 790-794.
[11] Santosh Kansal, Piyush Laad (2015), "Performance & Thermal Analysis of Heat Sink with Fins of Different Configuration using CFD", International Journal of Scientific & Engineering Research, 6 (6), PP: 1487-1495.
[12] Ravi Teja (2015), "Optimization of Heat Transfer through Rectangular Duct", International Research Journal of Engineering and Technology", 2 (4), PP: 1906-1910.

[13] Priyank Lohiya, Shree Krishna Choudhary (2015), "Numerical Study on Heat Transfer of Turbulent Duct Flow through Ribbed Duct", International Journal of Engineering Sciences & Research Technology, 4 (7), PP: 178-182.

[14] Vivek Rao, Dr. Ajay Gupta, Amit Kumar (2015), "CFD Based Heat Transfer Analysis of Solar Air Heater Duct Provided with Artificial Roughness", International Journal of Scientific & Engineering Research, 6 (5), PP: 28-35.

[15] Ashok Singh Yadav, Tarun Singh Samant, Lokesh Varshney (2015), "A CFD Based Analysis of Solar Air Heater Having V-Shaped Perforated Blocks on Absorber Plate", International Research Journal of Engineering and Technology", 2(2), PP: 822-829.

[16] Skullong S., Thianpong C. and Promvonge, P., 2015, Effects of rib size and arrangement on forced convective heat transfer in a solar air heater channel, Heat and Mass Transfer, pp. 1-11.

[17] Arkan Al-taie, Hasasn Ali Jurmut (2014), "Experimental and Numerical Investigation of Convective Heat Transfer in a Circular Tube with Internal square ribs", Journal of Babylon University/Engineering Sciences, 4 (22), PP: 910-918.

[18] Mostafa M. Awad (2013), "Assessment of Convergent-Divergent Fins Performance in Natural Convection", Journal of American Science, 9 (2), PP: 116-124.

[19] Raj Kumar (2013), "CFD based analysis of Heat Transfer and Friction Characteristics of Broken Multiple Rib Roughened Solar Air Heater Duct", International Journal of Mechanical and Production Engineering Research and Development, 3 (5), PP: 153-160.

[20] Anil Kumara, Muneesh Sethia, Khushmeet Kumara (2013), "Computational Fluid Dynamics Based Analysis of Angled Rib Roughened Solar Air Heater Duct", International Journal of Thermal Technologies, 3 (7), PP: 43-47.

[21] Suman Saurav, V.N. Bartaria (2013), "CFD Analysis of Heat Transfer through Artificially Roughened Solar Duct", International Journal of Engineering Trends and Technology, 4 (9), PP: 3937-3944.